Rapid Communication

Orientation selectivity in luminance and color vision assessed using 2-d band-pass filtered spatial noise ☆

William H.A. Beaudot [1], Kathy T. Mullen *

McGill Vision Research, Department of Ophthalmology, McGill University, 687 Pine Avenue West, H4-14, Montréal, Québec, Canada H3A 1A1

Abstract

We evaluated orientation discrimination in color and luminance vision using an external noise paradigm. Stimuli were spatiotemporal patches of 2D orientation noise isolating the achromatic, red–green and blue–yellow mechanisms, and matched in multiples of contrast detection threshold. We found a monotonic increase of orientation discrimination thresholds with the stimuli orientation bandwidths that is similar for both color and luminance contrasts. This dependence was fitted with two suitable models. A variance summation model suggests that internal orientation noise is significantly greater for the chromatic than for the achromatic mechanisms, while the efficiencies are similar. A gain control model of orientation tuning suggests that both chromatic and achromatic mechanisms are characterized by broadly tuned orientation detectors and that the relative chromatic deficit in orientation discrimination may only result from a slightly broader orientation tuning for the chromatic mechanisms. The moderate deficiency in chromatic orientation discrimination may account for the small differences found in shape perception between color and luminance vision.
© 2004 Elsevier Ltd. All rights reserved.

Keywords: Human color vision; Orientation discrimination; Noise stimulus; Variance summation model; Gain control model

1. Introduction

Form vision depends on hierarchical cortical stages that are well established for luminance vision. In the first cortical stage the visual image is broken down piecemeal by neurons acting as arrays of orientation-selective and spatially band-pass filters. Subsequent stages involve integrative processes that link these local components to extract the salient features of the image, such as borders and contours. Integrative or global processes are also required to link local features, such as contours, curves or corners, into whole and identifiable shapes. It is now clear that color vision can support many aspects of 2-d form perception in its own right, a significant evolution of the earlier view-point that color vision had little shape processing apparatus of its own and simply filled in contours and boundaries primarily defined by luminance contrast (Livingstone & Hubel, 1987, 1988). For example, both red–green and blue–yellow cone opponent mechanisms can support a simple contour integration task based on the linking of locally oriented Gabor patches across space with chromatic performance on this task falling marginally below that for luminance contrast (Beaudot & Mullen, 2003; McIlhagga & Mullen, 1996; Mullen, Beaudot, & McIlhagga, 2000). For 2-d shape discrimination, both red–green and blue–yellow cone opponent processes are found to perform below luminance vision by about 2-fold for stimuli

equated in multiples of contrast threshold (Mullen & Beaudot, 2002). Thus although color vision can clearly support these orientation dependent and linkage based stages of form perception, there are some additional limitations on its performance not present for luminance vision.

As in any hierarchical system, performance deficits manifest at a higher stage may have been incurred at an earlier one. Thus in order to identify whether deficits of spatial processing for color vision genuinely originate at the higher stages of form vision, the lower stages must first be thoroughly understood. In particular, the earliest and most fundamental stage of form processing is the filtering of the visual image by arrays of orientationally (and spatially) selective filters. Since all higher aspects of form perception rely on this early orientation-selective processing stage, performance on higher spatial tasks may potentially be limited by the fidelity of the orientation information extracted from the image at this stage. Thus an understanding of the processing of orientation information in color vision relative to luminance vision is important for interpreting and modeling performance for higher spatial tasks, such as global shape perception.

Psychophysical studies have shown that color possesses the basic property of orientation sensitivity. Webster, De Valois, and Switkes (1990) investigated orientation discrimination and found a small deficit for color vision in comparison to luminance vision (about 1.5 times) maintained over the whole suprathreshold contrast range (Webster et al., 1990). Reisbeck and Gegenfurtner (1998) and Wuerger and Morgan (1999) found a similar effect, once their stimulus contrasts have been normalized to the respective detection threshold. In addition studies using adaptation (Bradley, Switkes, & De Valois, 1988) and sine-wave masking (Pandey Vimal, 1997) have found orientation-tuned mechanisms for red–green color vision; the masking study reported these to be more broadly tuned for color compared to luminance vision at the lower spatial frequencies (<2 cpd). In addition, psychophysical results have shown that red–green color vision has band-pass spatial filters similar in bandwidth to those for luminance vision (Bradley et al., 1988; Losada & Mullen, 1994, 1995; Mullen & Losada, 1999; Pandey Vimal, 1997).

In this paper we make a quantitative comparison between orientation discrimination for chromatic and luminance vision. We use a new method, based on an external noise paradigm developed from Heeley, Buchanan-Smith, Cromwell, and Wright (1997), that allows the assessment of orientation discrimination over a range of stimulus orientation bandwidths. This paradigm (and the underlying variance summation model) was originally developed to assess the internal noise and relative sampling efficiency of the mechanisms underlying contrast discrimination tasks (Pelli, 1990;

Pelli & Farell, 1999), and was subsequently applied to orientation discrimination. Stimulus orientation bandwidths can be considered as a source of external noise and are used in this model to evaluate the internal orientation noise and relative sampling efficiency of the underlying orientation-tuned mechanisms (Demanins, Hess, Williams, & Keeble, 1999; Heeley et al., 1997). Stimuli are constructed by filtering 2D Gaussian noise in the Fourier domain, and the task is to discriminate between two stimulus orientations in a staircase procedure to estimate orientation discrimination thresholds. The use of orientation noise allows orientation discrimination to be investigated under more ecologically valid conditions since natural stimuli are characterized by a broad-band distribution in several of their dimensions (spectral, spatial, temporal, etc.) and visual neurons are also characterized by broad tuning along these dimensions. To interpret the differences and similarities between luminance and chromatic mechanisms in orientation discrimination, we used two models, the variance summation model traditionally used in the external noise paradigm and a biologically plausible nonlinear model of orientation selectivity, both capable of predicting the dependence of orientation discrimination threshold on orientation bandwidth of noise stimuli.

2. Methods

2.1. Stimuli

Following Heeley et al. (1997), we measured orientation acuity for 2-dimensional band-pass filtered noise. The stimuli are constructed by filtering Gaussian noise in the Fourier domain with an appropriate anisotropic filter. The modulation transfer function of this filter is a Gaussian in radial frequency and radial angle. The spectral density of the resulting noise can be expressed in polar coordinates:

$$S_n(f_x, f_y) = G_r(f_r, f_o, \sigma_f) \cdot G_\theta(\theta, \theta_o, \sigma_\theta) \tag{1}$$

where

$$G_r(f_r, f_o, \sigma_f) = \exp\left[-\frac{1}{2} \cdot \left(\frac{f_r - f_o}{\sigma_f} \right)^2 \right] \tag{2}$$

$$G_\theta(\theta, \theta_o, \sigma_\theta) = \exp\left[-\frac{1}{2} \cdot \left(\frac{\theta - \theta_o}{\sigma_\theta} \right)^2 \right]$$
$$+ \exp\left[-\frac{1}{2} \cdot \left(\frac{\theta - (\theta_o + \pi)}{\sigma_\theta} \right)^2 \right] \tag{3}$$
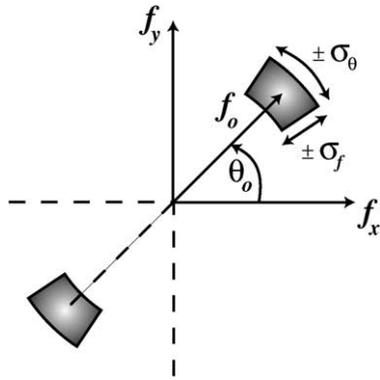
$$f_r = \sqrt{f_x^2 + f_y^2} \tag{4}$$

Fig. 1. Schematic Fourier representation of the spectral density of 2D oriented Gaussian noise.

and

$$\theta = \operatorname{atan}(f_y/f_x) \tag{5}$$

f_x and f_y are the cartesian spatial frequencies, f_r is the radial spatial frequency, f_o is the peak spatial frequency, σ_f is the frequency half-bandwidth, θ is the radial angle, θ_o is the peak orientation, σ_θ is the orientation half-bandwidth. Fig. 1 illustrates the extent and location of the noise spectral density in the Fourier domain.

After inverse Fourier transform, the filtered noise is multiplied by a spatial Gaussian envelope ($\sigma_{x,y} = 1°$) to obtain patches of orientation noise localized in space. Fig. 2 shows examples of the resulting noise stimuli, and illustrates the effects of increasing spatial orientation bandwidths. We used a low spatial peak frequency (f_o) of 1.5 cpd to avoid chromatic aberration artifacts for the isoluminant stimuli (Bradley, Zang, & Thibos, 1992). Spatial full-bandwidth ($2\sigma_f$) varied between 1/4 and 1 octaves, and orientation half-bandwidth (σ_θ) varied between 1° and 48°. The reference patch was vertical with a 5° jitter ($\theta_o = 90 \pm 5°$). Contrasts were matched in multiples of detection threshold (typically 10 times, see protocol section).

2.2. Chromatic representation of the stimuli

Three different stimuli were used that isolated the red–green (RG), blue–yellow (BY) and the luminance post-receptoral mechanisms respectively. [2] The chromaticity of the stimuli was defined using a 3-dimensional cone contrast space in which each axis represents the quantal catch of the L, M and S cone types normalized with respect to the white background (i.e., cone contrast). Stimulus chromaticity and contrast is given by a

---

[2] We use the color terms 'red–green' (RG) and 'blue–yellow'(BY) to refer to the two cone opponent mechanisms that combine the L and M cones, and the S with L and M cones, respectively. These mechanisms when activated individually by cardinal stimuli do not give rise to the unique color sensations of red, green, blue or yellow and so should not be confused with the perceptual color opponent processes.
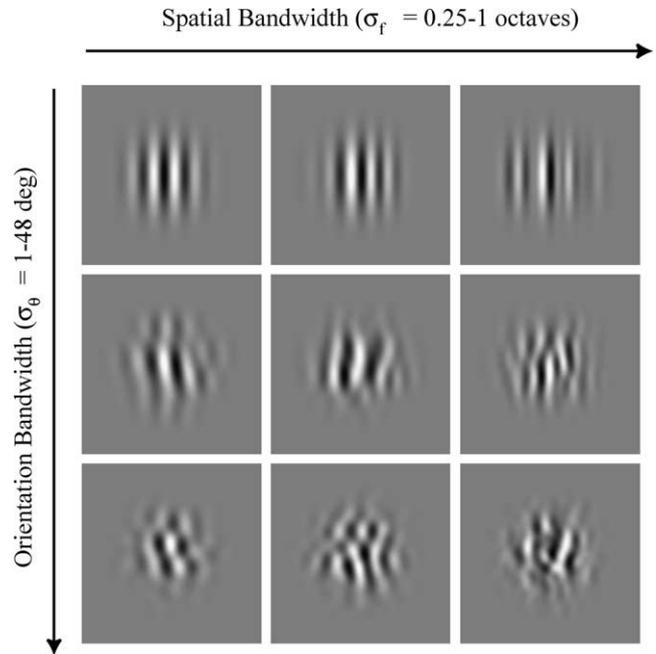
Spatial Bandwidth (σ_f = 0.25-1 octaves)

Fig. 2. Examples of noise stimuli: Gaussian-enveloped 2D noise as a function of spatial and orientation bandwidths.

vector direction and magnitude, respectively, within the cone contrast space, and so is device independent. Red–green, blue–yellow, and achromatic cardinal stimuli were determined within this space to isolate each of the three different post-receptoral mechanisms. A cardinal stimulus isolates one post-receptoral mechanism and is invisible to the other two, and is defined as the unique direction orthogonal in cone contrast space to the vector directions representing the other two post-receptoral mechanisms (Cole, Hine, & McIlhagga, 1993). We selected our cardinal stimuli from the knowledge of the cone weights of the three post-receptoral mechanisms provided by earlier studies (Cole et al., 1993; Sankeralli & Mullen, 1996, 1997). These studies have identified the relative cone weights of the mechanisms to be $L - M$ (the red–green mechanism), $S - 0.5(L + M)$ (the blue–yellow mechanism), and $xL + M$ (the luminance mechanism) where $x > 1$ and is variable between subjects. (Note that the symbols L, M and S represent the relative cone weights to the mechanisms within the cone contrast space.) From these cone weights the achromatic cardinal stimulus direction in the cone contrast space is $L + M + S$, the blue–yellow cardinal direction is the S-cone axis, and the red–green cardinal direction is $L - xM$. The wide inter-subject variability found for the luminance mechanism affects the specification of the isoluminant red–green cardinal direction. Red–green isoluminance (the value of x, above) was determined for each subject individually using a minimum motion technique (Cavanagh, Tyler, & Favreau, 1984) for a patch of grating (1.5 cpd, 3.6°²) viewed binocularly and foveally

and having the same mean luminance and chromaticity as the noise stimuli used in the main experiment.

2.3. Apparatus and calibrations

Stimuli were displayed on a Sony Trinitron monitor (GDM-F500R) driven by a VSG 2/4F graphics board (Cambridge Research Systems Ltd., Rochester, England) with 15 bits contrast resolution, housed in a Pentium PC computer. The frame rate of the display was 76 Hz. The spectral emissions of the red, green and blue guns of the monitor were calibrated using a PhotoResearch PR-650-PC SpectraScan (Chatsworth, CA). The monitor was gamma corrected in software with lookup tables using luminance measurements obtained from an OptiCAL gamma correction system interfaced with the VSG display calibration software (Cambridge Research Systems). The Smith and Pokorny fundamentals (Smith & Pokorny, 1975) were used for the spectral absorption of the *L, M* and *S* cones. From these data, a linear transform was calculated to specify the phosphor contrasts required for given cone contrasts (Cole & Hine, 1992). The monitor was viewed in a blacked out room. The mean luminance of the display was 60 cd/m^2. The stimuli were viewed at 60 cm. Stimuli were generated on-line, and a new stimulus was generated for each presentation.

2.4. Protocol

As orientation thresholds decrease with increasing suprathreshold stimulus contrast (Reisbeck & Gegenfurtner, 1998), it is critical to take the relative contrast sensitivities into account when comparing different post-receptoral mechanisms (Mullen & Beaudot, 2002; Mullen et al., 2000). Consequently all stimuli (RG, BY and Ach) were matched in multiples of the contrast detection threshold, measured using a temporal 2AFC staircase procedure. In each trial, one interval contained a test stimulus and the other contained a blank stimulus with the same average luminance. Subjects were asked to indicate which interval had the stimulus (noise patch). Orientation discrimination was measured using a temporal 2AFC staircase procedure, at 10 times the contrast detection threshold at three spatial bandwidths (σ_f = 0.25, 0.5 and 1 octaves) as a function of the orientation bandwidth (σ_θ = 1°–48°) of the stimuli. The orientation bandwidth, defined by a Gaussian distribution with standard deviation σ_θ, can be considered as a source of external noise used to explore the degree of selectivity of orientation tuning in the discrimination task. In each trial, the subject has to determine in which direction, clockwise or counter-clockwise, the patch of orientation noise in the second interval appeared to be rotated with respect to the first. One of the intervals contained a vertical reference patch with a 5° jitter, while

the other one contained another noise patch rotated by an amount depending on the staircase. Both patches were independently generated in each trial.

In both 2AFC staircase procedures, either the stimulus contrast or the stimulus orientation difference was reduced after two correct responses, and increased after one wrong response. The change was 50% before the first reversal, and 25% after the first reversal. Each session stops after six reversals, and the threshold corresponding to a criterion of 71% correct was computed from the mean of the last five reversals. The duration of each stimulus was 1 s, and the overall contrast of each stimulus was modulated in time up and down according to a temporal Gaussian envelop (σ_t = 250 ms) centered on the temporal window (1 s). Auditory feedback was given after each trial. A black fixation mark was briefly presented at the beginning of each session in the center of the display, and subjects were asked to sustain their focus during the whole session. Practice trials were run before the experiments commenced. The number of trials per session for each experiment was between 30 and 50 for each subject, and 4–5 sessions were performed for each condition.

2.5. Observers

The observers were the two authors (WB and KTM) and one naïve subject (MW). All three have normal, or refracted to normal vision, and all have normal color vision according to the Farnsworth-Munsell 100-Hue Test. All experiments were done under binocular conditions. Achromatic, red–green and blue–yellow contrast detection thresholds, respectively, were 1.3%, 0.8%, 4.7% for subject WB; 2%, 0.75%, 11.1% for subject KTM; and 2.1%, 0.9%, 5.7% for subject MW.

2.6. Data analysis

To make a quantitative comparison between orientation discrimination for chromatic and luminance vision, we analyze the experimentally measured orientation discrimination thresholds as function of the stimulus orientation bandwidth by fitting two different models to the data, the variance summation model and a biologically plausible nonlinear model. These two models are qualitatively similar since they both predict a monotonic increase of the thresholds with the increase of external noise, although they differ in their underlying assumptions and in the significance of their parameters (Beaudot & Mullen, in revision).

2.6.1. Variance summation model
The manner in which orientation acuity declines with stimulus bandwidth suggests it is determined by a summation of noise processes (Heeley et al., 1997; Pelli, 1990):

$$\sigma_{\mathrm{o}} = \sqrt{\sigma_{\mathrm{Int}}^2 + (\sigma_\theta^2/N)} \qquad (6)$$

According to this model, the psychophysical threshold is limited by both internal and external noise processes. These noise processes are assumed to be independent, thus their variances add. In this model, σ_{o} is the experimentally observed threshold, σ_{Int} the internal noise, σ_θ the external noise, and N is the sampling efficiency, which reflects how much of the stimulus is used for the task.

2.6.2. Nonlinear model

As a means of accounting for how the broad orientation bandwidth of psychophysical channels and orientation-tuned cortical cells could support hyper-acuity levels of orientation discrimination, it has been proposed that detection and discrimination are subserved by different mechanisms (Blake & Holopigian, 1985; Regan & Beverley, 1985). As illustrated in Fig. 3a this scheme relies on a bank of overlapping and broadly tuned orientation-selective filters with filter height indicating relative activity levels. The detection of oriented stimuli is subserved by the most active filter, which is centered on the stimulus peak orientation (Fig. 3b–c). On the other hand, orientation discrimination is subserved by neighboring filters, not centered on the stimulus peak orientation, whose responses are maximally modulated by orientation changes in the stimulus occurring along their flanks (Fig. 3d–e) where their slopes are the steepest (Scobey & Gabor, 1989). A direct consequence of this off-orientation looking strategy is that orientation discrimination may not be limited by the tuning bandwidth of the detection filter per se but by its sensitivity to orientation changes, and that depends on the shape of its tuning curve and its noise level. If this strategy is the basis of orientation discrimination, one would also expect that the ability to detect small changes in orientation is dependent on the orientation bandwidth of the stimulus, as this is found psychophysically with the external noise paradigm. In the model, small orientation changes in narrow-band stimuli should be optimal in modulating the response of the discrimination mechanism, that is by maximising its differential response, while similar orientation changes in broad-band stimuli should not be as effective, requiring larger orientation changes to elicit equivalent response. Such a dependence is obtained if the filter response decreases with the stimulus bandwidth as illustrated in Fig. 3c and e. We demonstrated in a recent study (Beaudot & Mullen, in revision) that a nonlinear interaction between the detection mechanism at the stimulus peak orientation and the neighboring mechanisms could achieve the monotonic dependence of orientation threshold on stimulus bandwidth.
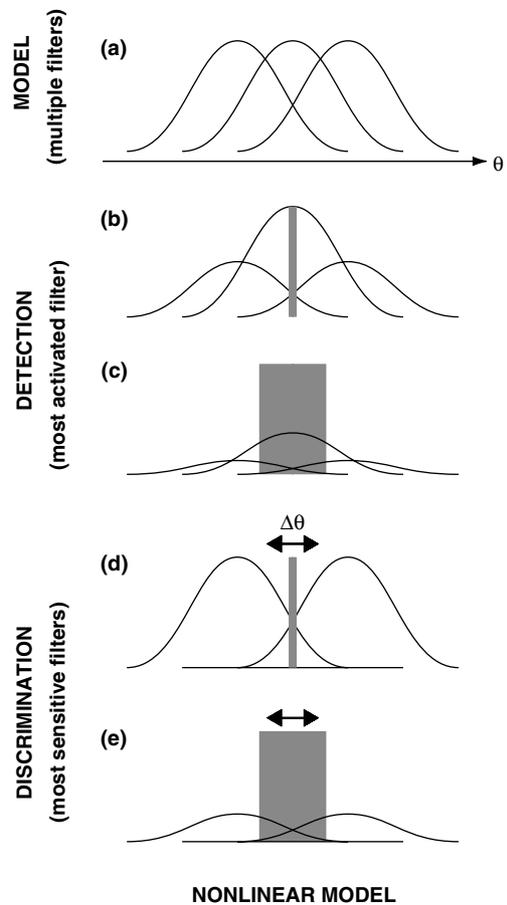

Fig. 3. Illustration of the off-orientation looking strategy as function of the stimulus orientation bandwidth. Profiles of three overlapping and broadly tuned orientation-selective filters are shown in figure a. The nonlinear filter responses for orientation detection are shown in figures b and c. The differential nonlinear filter responses for orientation discrimination are shown in figures d and e. The fine and thick grey bars in b–e represent narrow and broad oriented stimuli, respectively, centered on the middle filter. The responses of each filter are modulated according to the relative position of the stimuli and are represented by their height, enabling a comparison of the middle and neighboring filters' relative responses. The double-arrows in d and e represent an orientation shift $\Delta\theta$ in the discrimination task. Note that the differential response for the central filter is null as the stimulus and the filter profile have the same peak orientation.

This nonlinear model is based on a gain control mechanism in the orientation domain, and relies on a divisive suppression between broadly tuned orientation-selective inputs. Appendix A describes the basics of this nonlinear model, and more details can be found in Beaudot and Mullen (in revision). Orientation discrimination thresholds as function of stimulus bandwidth were derived by applying the ideal-observer theory to the differential responses of the nonlinear detector (Geisler & Albrecht, 1997; Scobey & Gabor, 1989). Only qualitatively similar to the variance summation model, the nonlinear model predicts a monotonic increase of orientation discrimination thresholds with the increase of external orientation noise.

3. Results

Fig. 4a–c shows the orientation thresholds measured for the three subjects as a function of external orientation noise for the three post-receptoral mechanisms and for the three spatial bandwidths. Each symbol represents the mean and standard deviation of the orientation threshold over 4–5 measurements. Consistent with the idea that stimulus orientation bandwidth acts as a source of external noise, orientation discrimination thresholds increased monotonically with stimulus bandwidth in all conditions and for the three post-receptoral mechanisms. The three subjects show this same pattern. The two models were fitted to the experimental thresholds using a least squares weighted procedure for each post-receptoral mechanism, each spatial bandwidth and each subject. Similar fits were obtained for the two models as shown in Fig. 4, with the variance summation model on the left column and the biologically plausible nonlinear model on the right column. We quantified the goodness of the fits with a Q measure given in the figures with a triplet for Ach, RG, BY, respectively. Q is a χ^2 distribution function which gives the probability that the minimum χ^2 is as large as it is purely by chance. For small Q values the deviation from the model is unlikely to be due to chance and the model may be incorrect. For larger Q values, the deviation from the model is more likely to arise by chance suggesting the model is an adequate description of the data. A Q of 0.1 suggests an acceptable model fit (Press, Teukolsky, Vitterling, & Flannery, 1992). The variance summation model provides a very good fit for all conditions ($Q > 0.3$), while the nonlinear model provides an acceptable fit in 20/27 conditions ($Q \geqslant 0.1$).

Under the variance summation model, estimates (mean and standard deviation) of the internal orientation noise (σ_{Int}) and relative sampling efficiency (N) were derived. In all subjects, there is no effect of spatial bandwidth on the internal noise, and the relative sampling efficiency shows a slight increase (by a factor of two) with the spatial bandwidth (0.25–1 octaves) in the three post-receptoral mechanisms. Spatial bandwidth has also no effect on the nonlinear model's parameters. Table 1 presents all parameters averaged across spatial bandwidths and subjects for each post-receptoral mechanism. Internal orientation noise is better for the achromatic mechanism ($\sigma_{Int} = 1.0 \pm 0.2°$) by a factor of about 1.5, with no difference between the two chromatic mechanisms ($\sigma_{Int} = 1.5 \pm 0.3°$ for RG, and $\sigma_{Int} = 1.5 \pm 0.1°$ for BY). Sampling efficiency is similar for the three post-receptoral mechanisms ($N = 34 \pm 4$). Overall, by fitting a variance summation model to the data, we found a moderate deficiency in orientation discrimination thresholds for the chromatic mechanisms, and no significant difference between the RG and BY mechanisms.

Under the nonlinear model, estimates of the orientation half-bandwidth of the excitatory and inhibitory components (σ_e, σ_i), the power law indices of these components (p, q), the gain factor of the inhibitory component (k), and the bandwidth ratio (σ_e/σ_i) were obtained. Table 1 shows that, according to this model, the three post-receptoral mechanisms have overall similar properties in terms of their averaged orientation bandwidths ($\sigma_e = 24.7 \pm 4°$, $\sigma_i = 37.9 \pm 4.2°$), averaged power law indices ($p = 0.95 \pm 0.07$, $q = 1.10 \pm 0.11$) and averaged inhibitory gain factor ($k = 201 \pm 38$). However a Student's t-test shows that the orientation bandwidth for the excitatory component differs significantly between the achromatic and both the chromatic mechanisms ($t = 2.5$, $P \leqslant 0.05$, df = 16 for ACH versus RG; $t = 2.8$, $P \leqslant 0.05$, df = 16 for ACH versus BY). The orientation bandwidths are slightly larger for the averaged chromatic mechanisms ($\sigma_e = 26.1 \pm 3.5°$) compared to the achromatic mechanism ($\sigma_e = 21.8 \pm 3.4°$), which is also supported by the significant difference in bandwidth ratio ($\sigma_e/\sigma_i = 0.56 \pm 0.08$ for ACH; $\sigma_e/\sigma_i = 0.7 \pm 0.1$ for RG and BY) ($t = 3.1$, $P \leqslant 0.01$, df = 16 for ACH versus RG; $t = 3.5$, $P \leqslant 0.01$, df = 16 for ACH versus BY). Consistent with the idea that the steepness of the tuning curve limits orientation resolution, this result suggests that the relative chromatic deficit in orientation discrimination, which is limited to a slightly higher internal noise, may result from a slightly broader orientation tuning that lowers the chromatic sensitivity to orientation discrimination.

4. Discussion

In this paper, we used an external noise paradigm to re-evaluate orientation selectivity in luminance and color vision. Previous studies have looked either at orientation acuity in discrimination tasks or at orientation tuning in detection tasks; their results are summarized in Tables 2 and 3, respectively. The studies that have looked at orientation discrimination (Table 2) have shown that the orientation acuities of the chromatic mechanisms are only slightly worse than that of the achromatic mechanism by a factor of less than two (Reisbeck & Gegenfurtner, 1998; Webster et al., 1990; Wuerger & Morgan, 1999). The present study is in perfect agreement, and also supports Webster et al.'s (1990) findings that RG and BY mechanisms have similar orientation acuity at high contrast. Not surprisingly, all these studies have used the same method for measuring orientation thresholds despite differences in stimulus properties.

Studies that have measured detection thresholds to estimate orientation tuning using adaptation and masking paradigms (Table 3) have reported similar or higher estimates of the orientation bandwidth of the red–green
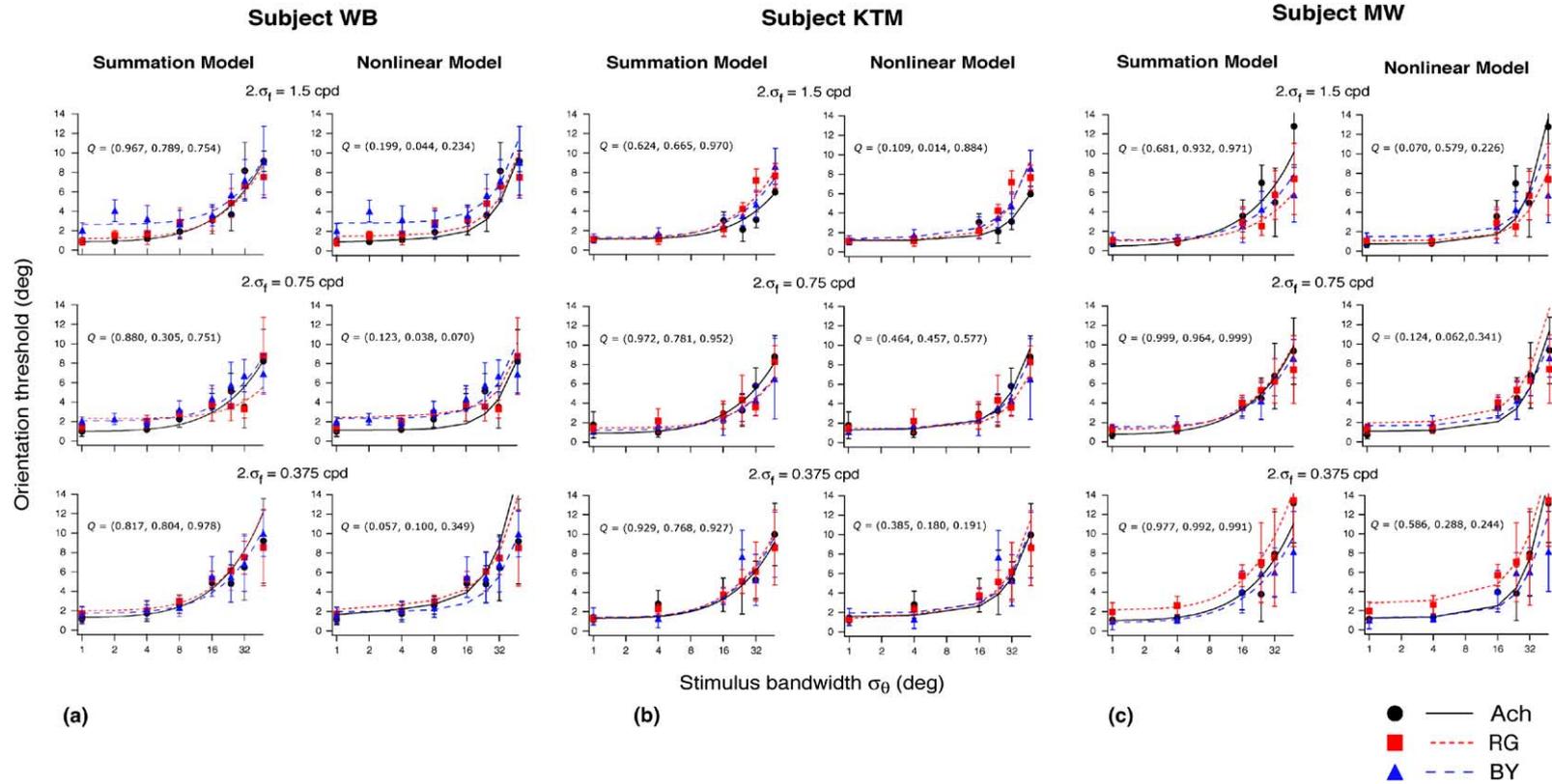
Fig. 4. a–c. Orientation discrimination threshold as a function of stimulus bandwidth (1–48°) and spatial bandwidth (0.25, 0.5 and 1 octaves) for the three post-receptoral mechanisms measured for the three subjects. The same data are fitted (solid and dashed curves) for each subject with two models, the variance summation model in the left panels for each subject and the biologically plausible nonlinear model in the right panels for each subject. Error bars denote standard deviations of the measurements. The Q triplets are a measure of goodness-of-fits for ACH, RG, BY stimuli, respectively (see text for details).

Table 1
Models' parameters

Models	Parameters	ACH	RG	BY
Variance summation model	σ_{Int} (deg)	1.0 ± 0.2	1.5 ± 0.3	1.5 ± 0.1
	N	30 ± 8	39 ± 17	33 ± 6
Biologically plausible nonlinear model	σ_e (deg)	21.8 ± 3.4	26.4 ± 4.4	25.8 ± 2.6
	σ_i (deg)	39.0 ± 4.6	38.0 ± 4.5	36.7 ± 3.5
	p	0.98 ± 0.07	0.94 ± 0.07	0.94 ± 0.07
	q	1.13 ± 0.13	1.11 ± 0.12	1.06 ± 0.09
	k	202 ± 38	185 ± 39	214 ± 35
	σ_e/σ_i	0.56 ± 0.08	0.70 ± 0.11	0.71 ± 0.10

Means and standard deviations of the models parameters across all conditions and all subjects: internal noise σ_{Int} and relative sampling efficiency (N) for the variance summation model; orientation half-bandwidth of the excitatory and inhibitory components (σ_e, σ_i), power law indices of these components (p, q), gain factor of the inhibitory component (k), and bandwidth ratio (σ_e/σ_i) for the nonlinear model.

Table 2
Discrimination tasks

Threshold	ACH	RG	BY	Stimuli
Webster et al. (1990)	0.65°	0.99°	0.99°	5° gratings 2cpd, HC, MDT
Reisbeck and Gegenfurtner (1998)	>for AC	>for MDT	NA	4° gratings 1cpd AC and MDT
Wuerger and Morgan (1999)	>for AC 1.0 ± 0.4	×2 for MDT	NA	0.2° × 0.6° Gabor 0.6–2cpd MDT (×10)
Present study (fit with the variance summation model)	1.0 ± 0.2	1.5 ± 0.3	1.5 ± 0.1	2° × 2° noise patch 1.5cpd MDT (×10)

Comparison of orientation discrimination thresholds (in degrees) obtained for the three post-receptoral mechanisms in previous studies and the present one. MDT: multiple of detection threshold; HC: high contrast; AC: absolute contrast; NA: not available.

Table 3
Detection tasks

Tuning	ACH	RG	BY	Methods and stimuli
Bradley et al. (1988)	45°	58°	NA	Adaptation gratings 2cpd
Pandey Vimal (1997)	50°–64°	60°–120°	NA	Masking D6 of Gaussian 0.5–2cpd
Present study (fit with nonlinear model)	44° ± 7	53° ± 9	52° ± 5	External noise 2° × 2° patch 1.5cpd, MDT (×10)

Comparison of orientation tuning (full-bandwidth in degrees) obtained for the three post-receptoral mechanisms in previous studies and the present one. MDT: multiple of detection threshold; D6: sixth derivative; NA: not available.

mechanism compared to the achromatic mechanism (Blake & Holopigian, 1985; Bradley et al., 1988; Pandey Vimal, 1997). To our knowledge, no psychophysical estimate of the orientation bandwidth of the blue–yellow mechanism has been reported so far. Fitting the nonlinear model to the orientation discrimination data has provided a way to estimate indirectly the orientation bandwidths of the underlying detectors (excitatory component σ_e) for each post-receptoral mechanism. As shown in Table 3, these estimates are consistent with the broad orientation bandwidths reported psychophysically for the achromatic and red–green mechanisms, and with the existence of a small difference in their bandwidths. Moreover the nonlinear model provides an estimate of orientation bandwidth for the blue–yellow mechanism similar to the orientation bandwidth for the red–green mechanism.

The variance summation model has the advantage of explicitly providing an estimate of the orientation inter-nal noise, while the nonlinear model does not. However the underlying assumptions of the variance summation model, such as additive noise and monotonic response, are not necessarily correct in the context of orientation processing (Beaudot & Mullen, in revision). On the contrary, the nonlinear model relies on physiologically plausible assumptions, such as multiplicative noise, broad orientation tuning, nonlinear interaction, and succeeds to account for the threshold elevation with external noise in orientation discrimination. This model predicts roughly similar orientation tuning of the underlying detectors for the three post-receptoral mechanisms. The predicted broad orientation bandwidths are similar to the broad bandwidths reported for cortical neurons (Blake & Holopigian, 1985; De Valois, Yund, & Hepler, 1982; Hammond & Andrews, 1978; Heggelund & Albus, 1978; Vogels & Orban, 1991), at least for their achromatic responses. Orientation selectivity in cortical neurons has primarily been associated with neurons

responsive to luminance-defined stimuli, and only non-oriented neurons have been thought to produce significant responses to purely chromatic stimuli (Lennie, Krauskopf, & Sclar, 1990). However there is large evidence that many neurons ($\approx$30%) are as responsive to luminance-defined and isoluminant red–green stimuli (Johnson, Hawken, & Shapley, 2001; Lennie et al., 1990; Thorell, De Valois, & Albrecht, 1984) and the only ones to show a chromatic orientation selectivity (Johnson et al., 2001). Moreover these color-luminance cortical neurons seem to show approximately equal orientation selectivity to both chromatic and luminance gratings (Johnson et al., 2001; Leventhal, Thompson, Liu, Zhou, & Ault, 1995). Our study provides further experimental and computational evidence of similar orientation processing for achromatic and chromatic stimuli. This could support the recent idea arising from both neurophysiological (Johnson et al., 2001; Lennie, 1998) and psychophysical (Clifford, Spehar, Solomon, Martin, & Zaidi, 2003; McIlhagga & Mullen, 1996, 1997; Mullen et al., 2000) evidence that the analysis of color and form is intrinsically coupled in the early cortical stages. The slight deficit in orientation discrimination we report for the chromatic mechanisms may account for the small differences we have found between color and luminance vision on contour integration and shape discrimination tasks (Beaudot & Mullen, 2003; Mullen & Beaudot, 2002).

Acknowledgments

Appendix A

The biologically plausible nonlinear model of the orientation-selective detector fitted to the experimental data is described by a modified Naka–Rushton equation (Beaudot & Mullen, in revision):

$$R(\theta_o) = \frac{r_e(\theta_o, \sigma_e)^p}{r_e(\theta_o, \sigma_e)^p + r_i(\theta_o, \sigma_i)^q} \tag{A.1}$$

where $r_e(\theta_o, \sigma_e)$ and $r_i(\theta_o, \sigma_i)$ are excitatory and inhibitory linear input stages in response to an orientation-defined stimulus $s(\theta, \theta_s, \sigma_\theta)$, defined respectively by

$$r_e(\theta_o, \sigma_e) = \sum_\theta g(\theta, \theta_o, \sigma_e) \cdot s(\theta) \tag{A.2}$$

$$r_i(\theta_o, \sigma_i) = k \cdot \sum_\theta g(\theta, \theta_o, \sigma_i) \cdot r_e(\theta)^p \tag{A.3}$$

$$s(\theta, \theta_s, \sigma_\theta) = \lambda(\sigma_\theta) \cdot \exp(-[\theta - \theta_s]^2 / 2\sigma_\theta^2) \tag{A.4}$$

$$\lambda(\sigma_\theta) = [a + b \cdot \exp(-\sigma_\theta/c)]/(a + b) \tag{A.5}$$

Both excitatory and inhibitory input stages are characterized by a Gaussian tuning curve $g(\theta, \theta_o, \sigma)$ centered at orientation θ_o and with an orientation half-bandwidth σ (σ_e and σ_i, respectively). To be consistent with our psychophysical study, stimuli $s(\theta, \theta_s, \sigma_\theta)$ are also characterized by a Gaussian distribution centered at orientation θ_s, with an orientation half-bandwidth σ_θ, and scaled by a factor λ that takes into account the effect of normalizing the stimuli to the same maximum contrast on their Fourier peak amplitude (parameters a, b, and c were obtained by fitting this function to the Fourier peak amplitude of the actual stochastic stimuli as function of their orientation bandwidth σ_θ). Other parameters are k the gain factor of the inhibitory input, p and q the power law indices for the excitatory and inhibitory inputs respectively.

Orientation discrimination thresholds were derived by applying the ideal-observer theory to the differential response of the nonlinear orientation-tuned detector (Eq. (A.1)). Accordingly, the discrimination index d' (1.0 for 75% correct in 2AFC) is given by the signal-to-noise ratio in neural responses assuming multiplicative noise (variance proportional to the mean by a constant K, typically between 1.2 and 1.5) (Geisler & Albrecht, 1997; Scobey & Gabor, 1989):

$$d' = \frac{|\Delta \text{Mean}|}{\sqrt{\text{Average Variance}}} = \frac{|R(\theta + \Delta\theta) - R(\theta)|}{\sqrt{\frac{K \cdot R(\theta + \Delta\theta) + K \cdot R(\theta)}{2}}} \tag{A.6}$$

Orientation discrimination thresholds, $\Delta\theta$, were obtained by solving $d' = 1$ as function of stimulus orientation bandwidth or external orientation noise (σ_θ). The fitting procedure provides estimates of the orientation half-bandwidths of the excitatory and inhibitory input stages, σ_e and σ_i, respectively, and estimates of other model's parameters as well (p, q, k).

References

Beaudot, W. H. A., & Mullen, K. T. (2003). How long range is contour integration in human color vision? *Visual Neuroscience, 20*(1), 51–64.

Beaudot, W. H. A., & Mullen, K. T. (in revision). Orientation discrimination in human vision: Psychophysics and modeling. *Vision Research*.

Blake, R., & Holopigian, K. (1985). Orientation selectivity in cats and humans assessed by masking. *Vision Research, 25*(10), 1459–1467.

Bradley, A., Switkes, E., & De Valois, K. (1988). Orientation and spatial frequency selectivity of adaptation to color and luminance gratings. *Vision Research, 28*(7), 841–856.

Bradley, A., Zang, L., & Thibos, L. N. (1992). Failures of isoluminance caused by ocular chromatic aberration. *Applied Optics, 31*, 2109–2148.

Cavanagh, P., Tyler, C. W., & Favreau, O. E. (1984). Perceived velocity of moving chromatic gratings. *Journal of the Optical Society of America A, 1*, 893–899.

Clifford, C. W., Spehar, B., Solomon, S. G., Martin, P. R., & Zaidi, Q. (2003). Interactions between color and luminance in the perception of orientation. *Journal of Vision, 3*(2), 106–115.

Cole, G. R., & Hine, T. (1992). Computation of cone contrasts for color vision research. *Behavioural Research, Methods and Instrumentation, 24*, 22–27.

Cole, G. R., Hine, T., & McIlhagga, W. (1993). Detection mechanisms in *L*-, *M*-, and *S*-cone contrast space. *Journal of the Optical Society of America A, 10*(1), 38–51.

De Valois, R. L., Yund, E. W., & Hepler, N. (1982). The orientation and direction selectivity of cells in macaque visual cortex. *Vision Research, 22*(5), 531–544.

Demanins, R., Hess, R. F., Williams, C. B., & Keeble, D. R. (1999). The orientation discrimination deficit in strabismic amblyopia depends upon stimulus bandwidth. *Vision Research, 39*(24), 4018–4031.

Geisler, W. S., & Albrecht, D. G. (1997). Visual cortex neurons in monkeys and cats: detection, discrimination, and identification. *Visual Neuroscience, 14*(5), 897–919.

Hammond, P., & Andrews, D. P. (1978). Orientation tuning of cells in areas 17 and 18 of the cat's visual cortex. *Experimental Brain Research, 31*(3), 341–351.

Heeley, D. W., Buchanan-Smith, H. M., Cromwell, J. A., & Wright, J. S. (1997). The oblique effect in orientation acuity. *Vision Research, 37*(2), 235–242.

Heggelund, P., & Albus, K. (1978). Orientation selectivity of single cells in striate cortex of cat: the shape of orientation tuning curves. *Vision Research, 18*(8), 1067–1071.

Johnson, E. N., Hawken, M. J., & Shapley, R. (2001). The spatial transformation of color in the primary visual cortex of the macaque monkey. *Nature Neuroscience, 4*(4), 409–416.

Lennie, P. (1998). Single units and visual cortical organization. *Perception, 27*(8), 889–935.

Lennie, P., Krauskopf, J., & Sclar, G. (1990). Chromatic mechanisms in striate cortex of macaque. *Journal of Neuroscience, 10*(2), 649–669.

Leventhal, A. G., Thompson, K. G., Liu, D., Zhou, Y., & Ault, S. J. (1995). Concomitant sensitivity to orientation, direction, and color of cells in layers 2, 3, and 4 of monkey striate cortex. *Journal of Neuroscience, 15*(3 Pt 1), 1808–1818.

Livingstone, M. S., & Hubel, D. H. (1987). Psychophysical evidence for separate channels for the perception of form, color, movement, and depth. *Journal of Neuroscience, 7*(11), 3416–3468.

Livingstone, M. S., & Hubel, D. H. (1988). Segregation of form, color, movement, and depth: anatomy, physiology, and perception. *Science, 240*(4853), 740–749.

Losada, M. A., & Mullen, K. T. (1994). The spatial tuning of chromatic mechanisms identified by simultaneous masking. *Vision Research, 34*(3), 331–341.

Losada, M. A., & Mullen, K. T. (1995). Color and luminance spatial tuning estimated by noise masking in the absence of off-frequency looking. *Journal of the Optical Society of America A, 12*(2), 250–260.

McIlhagga, W. H., & Mullen, K. T. (1996). Contour integration with colour and luminance contrast. *Vision Research, 36*(9), 1265–1279.

McIlhagga, W. H., & Mullen, K. T. (1997). The contribution of colour to contour integration. In C. M. Dickenson, I. Murray, & D. Carden (Eds.), *Colour vision research: proceedings of the John Dalton conference* (pp. 187–196). London: Taylor & Francis.

Mullen, K. T., & Beaudot, W. H. (2002). Comparison of color and luminance vision on a global shape discrimination task. *Vision Research, 42*(5), 565–575.

Mullen, K. T., Beaudot, W. H., & McIlhagga, W. H. (2000). Contour integration in color vision: a common process for the blue–yellow, red–green and luminance mechanisms? *Vision Research, 40*(6), 639–655.

Mullen, K. T., & Losada, M. A. (1999). The spatial tuning of color and luminance peripheral vision measured with notch filtered noise masking. *Vision Research, 39*(4), 721–731.

Pandey Vimal, R. L. (1997). Orientation tuning of the spatial-frequency-tuned mechanisms of the red–green channel. *Journal of the Optical Society of America A, 14*(10), 2622–2632.

Pelli, D. G. (1990). The quantum efficiency of vision. In C. B. Blakemore (Ed.), *Vision: coding and efficiency* (pp. 3–24). Cambridge: Cambridge University Press.

Pelli, D. G., & Farell, B. (1999). Why use noise? *Journal of the Optical Society of America A, 16*(3), 647–653.

Press, W. H., Teukolsky, S. A., Vitterling, W. T., & Flannery, B. P. (1992). *Numerical recipes in C: the art of scientific computing.* Cambridge: Cambridge University.

Regan, D., & Beverley, K. I. (1985). Postadaptation orientation discrimination. *Journal of the Optical Society of America A, 2*(2), 147–155.

Reisbeck, T. E., & Gegenfurtner, K. R. (1998). Effects of contrast and temporal frequency on orientation discrimination for luminance and isoluminant stimuli. *Vision Research, 38*(8), 1105–1117.

Sankeralli, M. J., & Mullen, K. T. (1996). Estimation of the *L*-, *M*-, and *S*-cone weights of the postreceptoral detection mechanisms. *Journal of the Optical Society of America A, 13*(5), 906–915.

Sankeralli, M. J., & Mullen, K. T. (1997). Postreceptoral chromatic detection mechanisms revealed by noise masking in three-dimensional cone contrast space. *Journal of the Optical Society of America A, 14*(10), 2633–2646.

Scobey, R. P., & Gabor, A. J. (1989). Orientation discrimination sensitivity of single units in cat primary visual cortex. *Experimental Brain Research, 77*(2), 398–406.

Smith, V. C., & Pokorny, J. (1975). Spectral sensitivity of the foveal cone photopigments between 400 and 500 nm. *Vision Research, 15*(2), 161–171.

Thorell, L. G., De Valois, R. L., & Albrecht, D. G. (1984). Spatial mapping of monkey V1 cells with pure color and luminance stimuli. *Vision Research, 24*(7), 751–769.

Vogels, R., & Orban, G. A. (1991). Quantitative study of striate single unit responses in monkeys performing an orientation discrimination task. *Experimental Brain Research, 84*(1), 1–11.

Webster, M. A., De Valois, K. K., & Switkes, E. (1990). Orientation and spatial-frequency discrimination for luminance and chromatic gratings. *Journal of the Optical Society of America A, 7*(6), 1034–1049.

Wuerger, S. M., & Morgan, M. J. (1999). Input of long- and middle-wavelength-sensitive cones to orientation discrimination. *Journal of the Optical Society of America A, 16*(3), 436–442.